ORIGINAL RESEARCH

Quantification of Collateral Supply with Local-AIF Dynamic Susceptibility Contrast MRI Predicts Infarct Growth

Mira M. Liu, Niloufar Saadat, Steven P. Roth, Marek A. Niekrasz, Mihai Giurcanu, Timothy J. Carroll, Gregory A. Christoforidis

ABSTRACT

BACKGROUND AND PURPOSE: In ischemic stroke, leptomeningeal collaterals can provide delayed and dispersed compensatory blood flow to tissue-at-risk despite an occlusion and can impact treatment response and infarct growth. The purpose of this work is to test the hypothesis that inclusion of this delayed and dispersed flow with an appropriately calculated Local Arterial Input Function (Local-AIF) is needed to quantify the degree of collateral blood supply in tissue distal to an occlusion.

MATERIALS AND METHODS: Seven experiments were conducted in a pre-clinical middle cerebral artery occlusion model. Dynamic susceptibility contrast MRI was imaged and post-processed to yield quantitative cerebral blood flow (qCBF) maps with both a traditionally chosen single arterial input function applied globally to the whole brain (i.e. "Global-AIF") and a delay and dispersion corrected AIF (i.e. "Local-AIF") that is sensitive to retrograde flow. Leptomeningeal collateral arterial recruitment was quantified with a pial collateral score from x-ray angiograms, and infarct growth calculated from serially acquired diffusion weighted MRI scans.

RESULTS: The degree of collateralization at x-ray correlated more strongly with qCBF using the Local-AIF in the ischemic penumbra (R^2=0.81) than traditionally chosen Global-AIF (R^2=0.05). qCBF using a Local-AIF was negatively correlated (less infarct progression as perfusion increased) with infarct growth (R^2 = 0.79) more strongly than a Global-AIF (R^2=0.02).

CONCLUSIONS: In acute stroke, qCBF calculated with a Local-AIF is more accurate for assessing tissue status and collateral supply than traditionally chosen Global-AIFs. These findings support use of a Local-AIF that corrects for delayed and dispersed retrograde flow in determining quantitative tissue perfusion with collateral supply in occlusive disease.

ABBREVIATIONS: MRI = magnetic resonance imaging; DSC = dynamic susceptibility contrast; PCS = pial collateral score; MCAO = middle cerebral artery occlusion; MCA = middle cerebral artery; AIF = arterial input function; rCBF = relative cerebral blood flow; qCBF = quantitative cerebral blood flow

Received month day, year; accepted after revision month day, year.
From the Department of Radiology, Medical Physics (MML, TJC), Department of Interventional Radiology (NS, GAC), Department of Surgery and Large Animal Studies (MAN), and the Department of Statistics (MG), University of Chicago, Chicago, IL, USA; Department of Anesthesiology (SPR), University of Illinois, Chicago, IL, USA; Department of Radiology, Biomedical Engineering and Imaging Institute (Current affiliation MML), Icahn School of Medicine at Mount Sinai, New York, NY, USA; Mount Carmel Health Systems (Current affiliation GAC), Columbus, OH, USA.

The authors declare no conflicts of interest related to the content of this article
Please address correspondence to Mira M. Liu, PhD, Department of Radiology, Biomedical Engineering and Imaging Institute, Icahn School of Medicine at Mount Sinai, 1470 Madison Ave, 1st floor, New York, NY, 10029, mirabai.liu@mountsinai.org

SUMMARY SECTION

PREVIOUS LITERATURE: In acute ischemic stroke, development of compensatory blood flow through the leptomeningeal collateral arterial network can maintain blood to tissue-at-risk and slow the growth of an infarction of tissue. Further, success of flow augmentation to serve as a bridge to thrombectomy may be dependent on leptomeningeal collateralization. Difficulties of measuring blood flow in acute ischemic stroke with a traditional single Global-AIF DSC include overestimation of perfusion deficits and failure to include delayed and dispersed compensatory blood flow.

KEY FINDINGS: Local-AIF DSC that incorporated delayed and dispersed flow improved correlation of penumbral perfusion against collateral supply at x-ray and against infarct growth compared to Global-AIF DSC. Local-AIF is an important correction in DSC of acute stroke to include compensatory collateral perfusion distal to an occlusion, even for relative perfusion.

KNOWLEDGE ADVANCEMENT: These findings support use of a Local-AIF rather than a single Global-AIF to (1) calculate quantitative cerebral blood flow in tissue-at-risk, (2) reduce false hypoperfusion in DSC of large vessel occlusions, and (3) quantify the blood supplied to a compromised perfusion bed through the leptomeningeal arteries.

INTRODUCTION

In acute ischemic stroke where a major blood vessel feeding the brain becomes occluded, it is well known that the development of

compensatory blood flow through the leptomeningeal collateral arterial network (collateral supply) can maintain blood to tissue-at-risk and slow the growth of an infarction of tissue. Minimizing "door-to-needle time" between hospital arrival and treatment currently drives ischemic stroke triage/treatment protocols regardless of an individuals' collateral supply. However, neuroprotection/bridge therapies which enhance collateral supply for "drip-and-ship" cases before transfer for specialized intervention, and "wake up strokes"[1] with unknown time of onset, may benefit from accurate quantification of collateral supply[2]. Further, the patient-to-patient variability of collateral supply contributes to unwanted variability of perfusion-diffusion mismatch, a measure used to predict positive outcomes in patients undergoing thrombectomy[3]. As previous studies have observed a slowing of infarct growth with flow augmentation therapies[4,5], and that the benefit of flow augmentation may be reduced in a setting of robust collateralization[6,7], accurate quantification of collateral supply is needed to identify if blood supply is sufficient to maintain viability, and determine if blood supply can be therapeutically enhanced to serve as a "bridge" to thrombectomy, and provide more accurate prediction of infarct growth.

Collateral supply can be estimated by x-ray digital subtraction angiography, single-photon emission computed tomography perfusion, computed tomography perfusion, and magnetic resonance perfusion[1] via prolonged Tmax[8] from dynamic susceptibility contrast (DSC). However, difficulties measuring perfusion as absolute cerebral blood flow (CBF) with traditional DSC include highly variable compensatory vasodilation of cerebral blood volume (CBV)[9] and deconvolution of a traditionally chosen single Global arterial input function (Global-AIF) overestimating perfusion deficits[10]. While using Global-AIF assumes a more uniform input function for ease of computation, use of a more complex Local-AIF allows one to correct for the delay and dispersion of the contrast bolus in every voxel when calculating CBF thereby providing a more accurate map of CBF.

This study investigates if qCBF calculated using a Local-AIF may reflect compensatory blood supply to tissue-at-risk of infarction more accurately than traditional DSC deconvolution analysis (Global-AIF). Using a standard MRI acquisition sequence in a preclinical animal model of ischemic stroke we post-processed DSC with both (1) a traditional Global-AIF[11], and (2) an automatically generated voxel-wise "Local-AIF" that corrects for delay and dispersion of the contrast bolus within every voxel. We hypothesized that quantification of perfusion calculated with an appropriate Local-AIF would correlate with degree of collateral supply to a perfusion bed distal to an occlusion and better predict infarct growth.

MATERIALS AND METHODS

Experimental Protocol

All experiments were conducted using a preclinical canine model of ischemic stroke[5,9,12-14]. The two-day experimental protocol was approved by the University of Chicago Institutional Animal Care and Use Committee and reported in compliance with ARRIVE guidelines. In this study, a series of 7 purpose bred adult canines (mean age = 4.1±2.9y, mean weight = 25.8±3.7kg, 6 female, 1 male) underwent permanent endovascular MCAO via embolic occlusion coils at the M1 segment proximal to the bifurcation (Appendix A1. Stroke Model). Subjects underwent x-ray arteriography, MRI DSC perfusion and serial quantification of infarct volume by DTI and were euthanized either the same evening or the following day.

Pial Collateral Score via X-ray Arteriography

Collateral supply was quantified 30 minutes post-MCAO by assessing X-ray arteriographic images (OEC9800; General Electric Healthcare, Chicago, IL) with a pial collateral score (PCS)[13-15]. PCS is an ordinal score from 1-11, developed for this preclinical model from a score of 1-5 for humans[15]. The scores were evaluated blinded to MRI qCBF by a neurointerventional radiologist with over 20 years of experience with human angiography and over 15 years with angiography in this canine model. Scoring was based on the delay and extent of retrograde filling of arterial branches distal to the occluded artery, with 1 being minimal/no collateralization and 11 being retrograde reconstitution of the collateral network up to the occlusion (Appendix A2. Pial Collateral Score). Subjects with PCS ≤ 8 were considered "poor" and PCS ≥ 9 considered "good" collateral supply, determined by previous study showing "poor" collaterals with core-infarct growing rapidly by assessment at the 2-hour time point and "good" collaterals still having a large volume of tissue-at-risk[14].

MR Acquisition

All MRI scans were performed on a 3T MRI scanner (Ingenia Philips, Cambridge, MA) with canines in a head-first, prone position using a 15 channel receive-only coil. DSC perfusion images were acquired 2.5 hours after occlusion (2D Gradient echo, T2*-weighted EPI, FOV=160 x160mm/matrix =176x176, 5 slices/6mm thick, TR/TE=500/30, 120 phases, total scan time = 60s)/ Rapid, 15s T1 maps were acquired using a 2D Inversion recovery Look Locker scan with a single-shot EPI readout (slice thickness = 6mm, FOV = 160 x 160 mm/matrix = 176 x 176) for the T1-bookend method. Gadolinium (Gd)-based contrast agent (Multihance, Bracco, Princeton, NJ, USA) was injected in the forepaw followed by a saline flush (Gd: 3mL at 2mL/s, saline: 20mL at 2mL/s).

Diffusion tensor images (DTI) were acquired at 30-minute intervals to calculate mean diffusivity (MD) post-MCAO for measuring infarct volume growth over time. A stack of 50 2D DTI was prescribed to cover the entire head (slice thickness= 2mm FOV =128x128 mm/matrix = 128x128, TR/TE = 2993/83ms, FA = 90°, b-values = 0, 800 s/mm^2, 32 directions). MD, rather than ADC, maps were used as DTI was acquired to study separate aspects of this model beyond the scope of the current study; for the purposes of detecting infarct in this study the sequences are treated as equivalent.

Traditional Global-AIF DSC Post-Processing

For traditional DSC, the single Global-AIF was chosen automatically based on a simultaneous assessment of early arrival time, narrow bolus, and large area under the concentration curve[16]. qCBF was calculated using the T1-bookend method[17] where T1(in ms) changes in the parenchyma and blood-pool are input to a two-compartment model[18-20] that yields qCBF (in ml/100g/min) including intra- to extra-vascular water exchange[19]. This T1-bookend method has undergone extensive validation[9,10,21], is fully automated to minimize user bias[20], and is available for use[22,23]. Deconvolving the voxel-wise parenchymal tissue curves against the Global-AIF yields mean transit time

(MTT) values for the calculation of qCBF using the central volume principal,

$$qCBF(ml/100g/min) = \frac{qCBV(ml/100g)}{MTT(min)}$$

In the remainder of this manuscript, we refer to these values as "Global-AIF qCBF" with Tmax calculated as the time at which the residue function reaches its maximum after deconvolution with the Global-AIF[24].

Local-AIF DSC Post-Processing

In a setting of vascular occlusion, the traditional Global-AIF as a global estimate of the contrast bolus shape as it enters the brain has been shown to overestimate the degree of hypoperfusion in vascular beds fed via collateral supply[11]. To address this shortcoming, a Local-AIF was automatically generated for every voxel within the deconvolution analysis of DSC perfusion to yield a map of qCBF in ml/100g/min. This Local-AIF was calculated using a previously reported technique[10],

$$Local\text{-}AIF(t) = Global\text{-}AIF(t) \otimes \frac{\alpha}{(\Delta t + 1)} e^{-\frac{\beta t}{\Delta t}}$$

which includes correction for delayed arrival time (Δt) and bolus dispersion ($\otimes e^{-\frac{\beta t}{\Delta t}}$) prior to arrival in the vascular bed with β determined individually from comparison to between Global-AIF and venous outflow (Appendix A3. Local-AIF Model). The Local-AIF is patient dependent and has been previously validated[9,10,21] in humans, and is available for use[22,23]. A prior study supports the Local-AIF accounting for both antegrade flow through a tight flow-limiting stenosis, cross-filling through Circle of Willis communication, and retrograde blood supply through collateral vascular networks when calculating perfusion[10].

Territories of Interest

Three physiologically relevant territories were operationally defined: (1) diffusion positive core (core infarct), (2) hypoperfused yet viable (tissue-at-risk) in the ipsilateral middle cerebral artery (MCA) territory and (3) contralateral normal hemisphere MCA territory. All territories were defined to being within the MCA territory across three consecutive 6 mm coronal slices starting at, and posterior to, the M1 segment. The core infarct and tissue-at-risk territories were selected by thresholding MD from DTI and Tmax calculated from DSC images using a Global AIF.

Core infarct was defined, as previously reported[12,13], as MD < $5.7e^{-4}$ mm^2/s^6, converted to binary infarction maps, and used to calculate infarct volumes. Infarction maps taken 2.5 hours post-MCAO were co-registered to DSC (MATLAB 2021b, The MathWorks, Natick, MA) for analysis of the perfusion deficit within and around the core infarct.

Tissue-at-risk (i.e. the ischemic penumbra) was defined as having prolonged Tmax relative to the Global-AIF (Tmax > 1.0s), but not yet infarcted (i.e., MD>$5.7e^{-4}$ mm^2/s). Tmax[25,26] thresholds for "hypoperfusion" established in larger, human brains may not be appropriate in canines. Therefore, this study's threshold of Tmax>1.0s encompassed all tissue potentially at risk with delayed arrival. These Global-AIF Tmax maps, minus the binary infarction maps, were applied to both Global-AIF qCBF and Local-AIF qCBF maps as binary masks to measure qCBF in "tissue-at-risk". Contralateral MCA territory was selected on the same three slices based on visible anatomical cues. Perfusion beds in the ipsilateral hemisphere that were not "at-risk" or core-infarct were not evaluated in analysis.

Statistical Analyses

Wilcoxon signed-rank, boxplots, and scatterplots (linear regression and Bland-Altman) were used to compare tissue qCBF as calculated with a Global-AIF and Local-AIF. Local-AIF qCBF, Global-AIF qCBF, and the difference between the two (ΔqCBF= Local-AIF qCBF – Global-AIF qCBF) were correlated against reference standard x-ray angiographic PCS with linear regression and spearman's rank. To examine how relative CBF (rCBF) would be impacted by AIF selection, rCBF was calculated as the ratio of tissue-at-risk to contralateral middle cerebral artery territory. As robust collateral supply would maintain homeostasis and slow infarct growth, Local-AIF qCBF and Global-AIF qCBF distal to the occlusion were correlated against infarct growth via linear regression. Local-AIF and Global-AIF qCBF were calculated in ml/100g/min within territories of interest (infarcted, tissue-at-risk, contralateral) and compared via Wilcoxon signed-rank. Wilcoxon rank sum was used to compare Local-AIF and Global-AIF qCBF in tissue-at-risk for cases with poor collaterals against cases with good collaterals. To investigate potential influence of AIF selection the difference in quantitative CBV (ΔqCBV=Local-AIF CBV – Global-AIF CBV) was compared as a function of collateral score.

The bootstrap z-test was used to estimate effect size for power calculation. All statistical analysis was performed in R (Rstudio 3.6.1, Posit PBC, Boston, MA USA, 2019) and Python 3.11.4 (Anaconda Inc., 2024) with statistical significance determined at the p = 0.05 level.

RESULTS

Access to all results, raw images and tabulated data is available upon request to the corresponding author. 83% of the parent study experiments were 'successful' and performed to completion, i.e. physiologic parameters maintained as planned and no complications such as procedural related vessel perforation; success rate improved over time and reached 100% success for the most recent nine consecutive experiments of the parent study (this current study analyzed only successful controls of the parent study). Representative parametric qCBF maps of a left MCAO calculated with a Global-AIF and a Local-AIF for subjects with (A, B) poor collateral supply (PCS=8) and (C, D) good collateral supply (PCS=11) are shown in Fig. 1. The observed differences in qCBF between A and B, as well as between C and D, result exclusively in post-processing from the choice of AIF (Global vs Local); identical DSC images and territory ROIs were used for A-B and for C-D. The corresponding 1-hour infarct and 4-hour infarct of the two cases in Fig. 1 are shown in Fig. 2 as mean diffusivity images. Visual inspection of Fig. 1 demonstrates that the presence of robust collateral supply (PCS=11) effectively mitigates the formation and growth of an infarct (Fig. 2, yellow arrows).

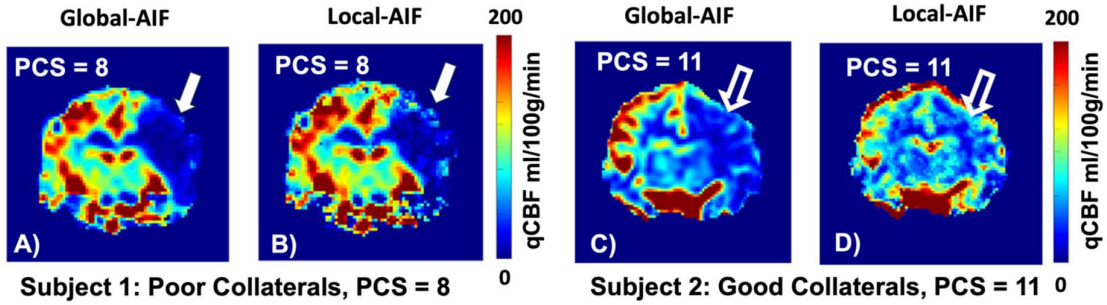

Figure 1**:** Coronal projection parametric qCBF maps in ml/100g/min. A) Poorly collateralized subject (PCS=8), using a single Global-AIF. B) The same subject/images post-processed using voxel-wise Local-AIF. Note the severe hypoperfusion (deep blue, denoted by arrow) in the poor collateral supply case, which persists when using a Local-AIF. C) A subject with robust collateralization (PCS =11) shown with a Global-AIF used to calculate qCBF and D) the same subject/images using Local-AIF to calculate qCBF. Note the markedly higher perfusion values (hollow, white arrow) attributable to the use of a delay and dispersed Local-AIF.

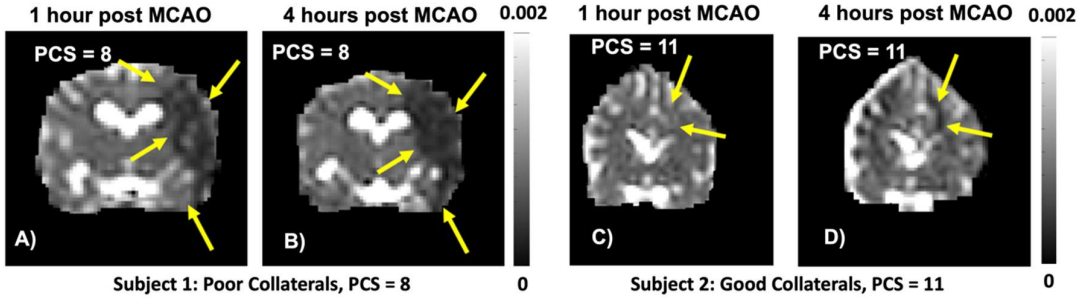

Figure 2: Coronal projection parametric mean diffusivity images acquired 1 and 4 hours after coil deployment in the left MCA. These are corresponding diffusion weighted images from the experiments displayed in Fig. 1 with A-B) poor collateral supply and C-D) good collateral supply. Note that robust collateralization results in significantly slower growing, and smaller infarction (yellow arrows).

Collateral Supply

Local-AIF qCBF values in the tissue-at-risk were more strongly correlated (Fig. 3A, $R^2 = 0.81$) with PCS than traditional Global-AIF DSC (Fig. 3B, $R^2 = 0.05$). This was also true for Spearman's rank correlation (Local-AIF statistic = 0.87, p = 0.01; Global-AIF statistic = 0.34, p = 0.45). The difference between Local-AIF and Global-AIF qCBF, (ΔqCBF= $CBF_{LOCAL\text{-}AIF}$ - $CBF_{GLOBAL\text{-}AIF}$) was moderately positively correlated with PCS ($R^2 = 0.49$).

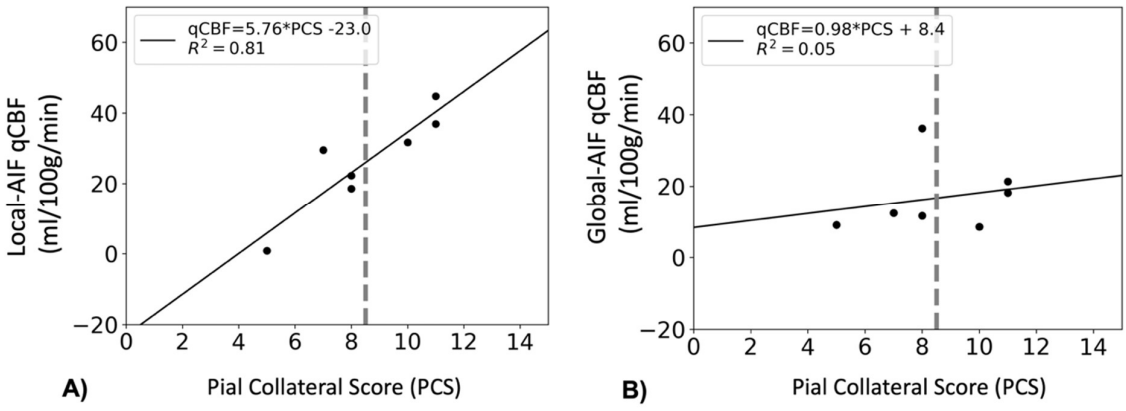

Figure 3: Scatter plots of tissue qCBF in ml/100g/min vs pial collateral score (PCS) within the operationally defined ischemic penumbra reconstructed with A) a Local-AIF and B) a traditional Global-AIF. Note: qCBF values are quantitative, values above ~18 ml/100g/min have sufficient flow to slow infarct growth.

Infarct Growth

qCBF calculated using the Local-AIF algorithm in the tissue-at-risk was strongly negatively correlated with infarct growth (higher local

CBF = slower infarct growth; Fig. 4A, R^2=0.79). In comparison, qCBF values calculated using a Global-AIF were consistently lower than Local-AIF values and did not correlate well with infarct growth (Fig. 4B, R^2=0.02).

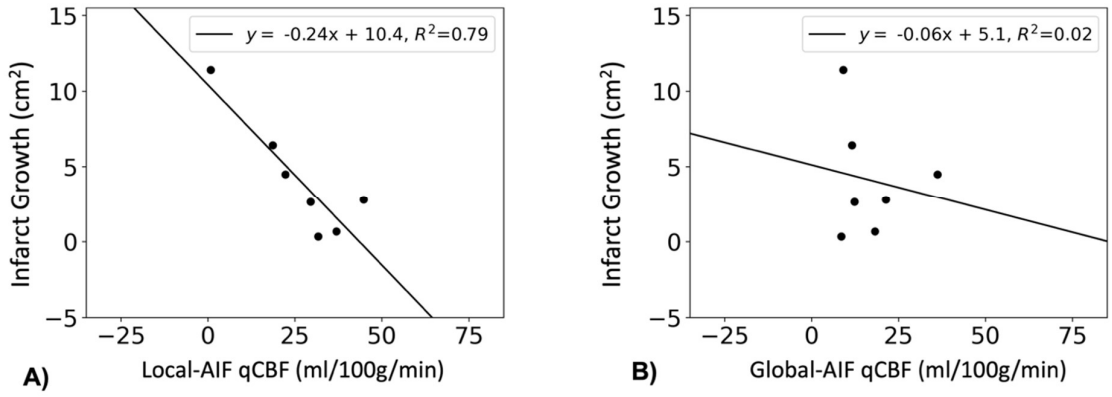

Figure 4: In the ischemic penumbra (MD>5.7× 10^{-4} mm^2/s, Tmax>1.0) A) qCBF calculated using a Local-AIF more strongly correlates with slower infarct growth whereas B) qCBF from a traditionally chosen Global-AIF is less predictive of infarct growth in the acute phase of an ischemic stroke.

Comparison in Territories of interest

A comparison between traditional Global-AIF and delay and dispersion corrected Local-AIF qCBF in ml/100g/min is shown as boxplots in Fig. 5. Median qCBF of the core infarct (Fig. 5A, MD<5.7$x10^{-4}$ mm^2/s), tissue-at-risk (Fig. 5B, MD>5.7$x10^{-4}$ mm^2/s and Tmax > 1.0 s), and the contralateral hemisphere MCA (Fig. 5C) are included. In the infarcted core both Global and Local-AIF showed qCBF values below the threshold for cell death from a study in primates (gray band < 18 ml/100g/min provided for context to the quantitative value this study calculated)[27]. In the tissue-at-risk, the CBF of "good" collaterals (PCS≥ 9, n=4) and "poor" collaterals (PCS≤ 8, n=3) is presented separately and color-coded to highlight the sensitivity of the Local-AIF to collateral supply (Fig. 5B).

Statistical comparison with Wilcoxon signed rank are shown in Table 1. Median qCBF in ml/100g/min from Local-AIF and Global-AIF were not statistically significantly different in the core infarct. In the tissue-at-risk, Local-AIF and Global-AIF were not significantly different for poor collaterals. However, for good collaterals, Local-AIF was higher than Global-AIF qCBF by +26.0ml/100g/min (p = 0.06), raising the average qCBF above the ischemic threshold. Further, the Local-AIF qCBF was an average +25.9ml/100g/min higher for subjects with good collaterals compared to Local-AIF of poor collaterals (rank sum statistic = -2.2, p=0.03) while Global-AIF qCBF of good and poor collaterals were not significantly different (Fig. 5B).

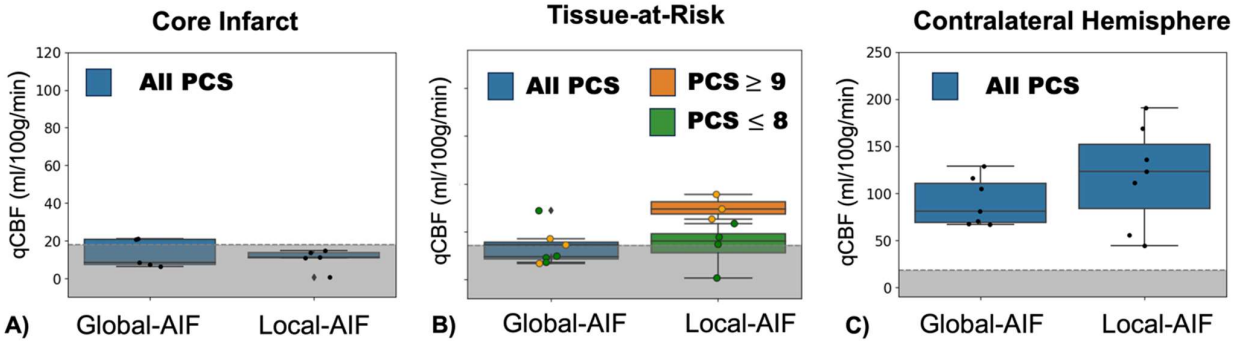

Figure 5: Boxplots of CBF in A) the core of an infarct, B) the penumbral tissue-at-risk, and C) contralateral, unaffected hemisphere. Local-AIF qCBF in tissue-at-risk is separated into good collaterals (PCS>8) and poor collaterals (PCS<8) by color and with scatter plots colored according to score. Contralateral qCBF is on a different range due to systemic compensatory mechanisms to include all data. The gray band represents qCBF values below 18 ml/100g/min, the ischemic threshold for neuronal death in primates.

Table 1: Differences between Local-AIF and Global-AIF DSC (ΔqCBF=Local-AIF qCBF – Global-AIF qCBF) in the three territories of interest, with all collateral scores dichotomized into good and poor. Statistical significance at the p = 0.10 level is denoted with *. The underestimation of CBF values using a single Global AIF compared to a voxel-wise local AIF (ΔqCBF) is greater when collateral supply is robust, but not significant in a setting of poor collateral supply; this is especially prevalent in tissue-at-risk.

	ΔqCBF Dichotomized by Collateral Score **Mean Difference (ml/100g/min) [Wilcoxon signed rank statistic, p-value]**		
	Core Infarct	Tissue-at-risk	Contralateral Hemisphere
All PCS	+2.26[11.0, p = 0.68]	+14.3[5.0, p = 0.07] *	-30.06[16.0, p = 0.84]
Good PCS>8	+10.78[0.0, p = 0.125]	+25.96[0.0, p = 0.06] *	-89.2[2.0, p = 0.19]
Poor PCS<8	-9.08[1.0.0, p = 0.50]	-5.07[1.0, p = 0.50]	+68.60[1.0, p = 0.50]

DSC: dynamic susceptibility contrast, qCBF: quantitative cerebral blood flow, PCS: pial collateral score.

Relative CBF

In the contralateral hemisphere the Local-AIF qCBF was lower for good collaterals by -92.5ml/100g/min (rank sum statistic = 1.9, p=0.05). In other words, Local-AIF showed higher qCBF in tissue-at-risk and lower contralateral qCBF for subjects with robust collateral supply while Global-AIF showed lower qCBF in the tissue-at-risk and higher contralateral qCBF. As such, *relative* rCBF=tissue-at-risk/contralateral perfusion with a Local-AIF correlated to collateral score (R^2=0.62, spearman's rank statistic = 0.76, p = 0.04) while Global-AIF rCBF did not (R^2=0.04, spearman's rank statistic = 0.38, p=0.40). The influence of Local AIF on qCBV was not significant.

Statistical Power

Regarding power analysis for sample size, difference in the slopes for prediction of infarct growth using Local-AIF (Fig. 4A) or Global-AIF (Fig. 4B) qCBF did not demonstrate statistical significance by the bootstrap z-test (z=-0.49, p = 0.62). However, R^2 values were significantly different (z=2.03, p = 0.04). In terms of power, the study was underpowered for both endpoints due to the sample size, with a minimum requirement of 41 subjects for ideal 80% power of both slope and R^2. However, the trend of improved slope and correlation with a Local-AIF remains (Fig. 4).

DISCUSSION

This study found that a voxel-wise "Local-AIF" that incorporates delay and dispersion of the bolus reflects the existence of compensatory collateral supply distal to an occlusion and predicts infarct growth better than a traditional single Global-AIF in DSC MRI. This suggests that a traditional Global-AIF without delay and dispersion correction does not include collateral supply and therefore may result in less accurate determination of hypoperfusion when robust leptomeningeal collateralization exists. These findings support use of a Local-AIF to (1) calculate qCBF using the previously reported "T1 bookend method"[9,17-21], (2) to image CBF supplied through the leptomeningeal arteries, and (3) more accurately predict of infarct growth in acute ischemic stroke.

When contrast agent is injected via IV, it travels through the heart and lungs and finally to the circle of Willis before perfusing the brain. In DSC MRI, the shape of contrast bolus upon entering the brain represents a Global-AIF. However, when there is an occlusion of a major artery, blood will have to travel around the occlusion to reach the infarcted hemisphere through the leptomeningeal collateral arterial network. The delay and the dispersion as blood travels through this collateral network can be corrected for with a Local-AIF. The Local-AIF presented in this work incorporates a term to account for the late arrival and the additional blunting of the bolus as it is propagated through the brain through the collateral network (Appendix A3. Local-AIF Model). The amount of delayed and dispersed blood that this Local-AIF corrects for was hypothesized to be directly related to the extent of collateralization of a subject.

Quantification of local qCBF distal to an occlusion using a Local-AIF demonstrated a strong correlation with the collateralization (i.e. PCS). Further, Local-AIF qCBF in the tissue-at-risk that would benefit most from robust collateral supply was reported above the threshold of 18ml/100g/min for subjects with good collaterals. Meanwhile, in the core infarct, as well as in tissue-at-risk for subjects with minimal collateral supply, Local-AIF showed no change in the degree of hypoperfusion. In other words, mathematically, the Local-AIF qCBF is the same as the Global-AIF qCBF when there is no delayed and dispersed arrival of the bolus through the collateral network ($Local\text{-}AIF_{\lim \Delta t \to 0} = Global\text{-}AIF$). This supports the automatic Local-AIF deconvolution analysis being applicable to all cases, irrespective of collateral supply, delayed antegrade flow, or circle of Willis cross filling.

Global-AIF qCBF demonstrated poor correlation to collateral supply, and no difference between good and poor collaterals, suggesting Global-AIF qCBF does not reflect the presence of collateral blood that is supplied, delayed and dispersed, through the leptomeningeal network. The absolute difference between the Global-AIF qCBF and the Local-AIF qCBF (ΔqCBF) correlated with PCS, further supporting Local-AIF including degree of collateral supply (vs slow antegrade stenotic flow) in an ischemic stroke. As both Global-AIF and Local- AIF use identical input images and regions of interest, the difference was only due to use of a voxel-wise delay and dispersion corrected Local-AIF. The effect of the Local-AIF was observed in relative perfusion as well. Local-AIF is an important correction in DSC of acute stroke to include compensatory collateral perfusion distal to an occlusion, even if the intent is for relative perfusion.

Previous study by Nael et al. (2018) of a perfusion collateral index demonstrated that good collaterals showed smaller volumes of severe hypoperfusion (arterial delay > 6s) and larger volumes of moderate hypoperfusion (arterial delay = 2-6s)[28]. While severe hypoperfusion with larger arterial delay represents tissue that is not receiving delayed compensatory flow, the moderate arterial delay may represent the delayed and dispersed flow through the collateral network. The current study supports quantifying this collateral supply as

qCBF by correction of delay and dispersion with a Local-AIF. Further, collaterals from the PCA and ACA territory may have differing timing in the superior and inferior division territories of the occluded MCA; this itself may affect the transit time and lead to qCBF requiring a Local-AIF to measure accurately.

Prior studies have reported correlation between infarct growth from both PCS and arrival time by DSC[14]. The current study provides a mechanistic validation for prior studies by indicating that subjects with higher Local-AIF qCBF, which includes contribution from collateral supply and corrected arrival time, observed slower infarct growth. The Local-AIF will improve prediction of infarction compared to Global-AIF as it can more accurately represent the perfusion in the tissue-at-risk, even if the perfusion is being supplied delayed and dispersed through the collateral network. Robust collateralization may have a longer window of treatment, particularly if collateral supply can be therapeutically enhanced, than an ischemic stroke case without robust collateral supply which must be treated immediately. As such, Local-AIF qCBF may be a predicter of infarct growth and provide insight into novel stroke therapeutic treatments[7].

Tmax, by definition, identifies the presence of delayed bolus arrival as prolonged Tmax and depicts malignant pattern used in acute stroke triage to identify patients who would benefit from immediate intervention[1]. The goal of this study was to quantify the leptomeningeal supply that mitigates infarct growth. The results suggest that Tmax can identify the *location* of delayed bolus arrival as tissue-at-risk, and that a Local-AIF can then *quantify* the local flow (i.e. degree of collateral supply) from the collateral network in that tissue-at-risk.

A previous study by Federau et al. (2019) has reported "local perfusion fraction" in acute stroke using non-contrast intravoxel incoherent motion (IVIM), with excitation and readout in the same plane, as a measure of collateral blood supply that traditional Global-AIF DSC cannot capture[29]. This current study demonstrated that traditional Global-AIF can be improved by correcting for the delay and dispersion to return the local perfusion. The correlation of Local-AIF qCBF to x-ray DSA PCS supported the ability of DSC to quantify 'local' collateral supply in ml/100g/min. In addition, as the influence of a Local-AIF on qCBV was not significant, the increased correlation with a Local-AIF was predominately due to the mean transit time component rather than the blood volume component. Since qCBF (in ml/100g/min) from a combination of the qCBV (with a T1 Bookend) and local mean transit time (with a Local-AIF) correlated with collateral supply and infarct growth, studies of local IVIM perfusion fraction[29] in acute stroke may benefit from an inclusion of mean transit time to quantify collateral supply[30].

This work was not without limitations. Use of a complex pre-clinical animal model limited the number of experiments that were run and vascular territories that were studied. We present a retrospective re-analysis of an animal model that designed to study flow augmentation in MCAO and was not powered for study of more subtle Local- vs Global-AIF qCBF differences between groups. This MCAO model and use of contrast afforded a limited number of perfusion measurements; a method that allows dynamic assessment of perfusion over the course of infarct development could be beneficial[29,30]. Co-registration and resampling were required for mapping of core-infarct and tissue-at-risk enabling imperfect co-registration of perfusion and diffusion images; images were analyzed region-by-region, rather than voxel-by-voxel. Translation of conclusions derived from animal-based models is a potential limitation; however, an MCAO model reduces error in evaluating methods for CBF calculation by allowing from more accurate assessment of occlusion time and comparison of subjects at multiple time points under similar physiologic conditions which is not possible in humans. The limited number of subjects used in this study limits statistical interpretation and significance. Additional studies are planned and underway in humans to examine translation from a canine model to humans. While time of reconstruction of Local-AIF qCBF maps is not prohibitive and it could be incorporated into existing analysis at the scan consul, "time-to-needle" constraints remain for clinical use of MRI in acute stroke; the automatic voxel-wise Local-AIF may have more clinical value as an adaptation in CT perfusion deconvolution.

CONCLUSIONS

When there is an occlusion of a major artery, the delay and dispersion as blood and contrast travels around the occlusion via the collateral network can be corrected for to capture collateral supply with a Local-AIF. By using a Local-AIF to calculate qCBF, the collateral supply was quantified, correlated with PCS, and was predictive of infarct growth. These findings support use of a Local-AIF rather than a single Global-AIF to (1) calculate qCBF in tissue-at-risk, (2) reduce false hypoperfusion in DSC of large vessel occlusions, and (3) quantify the blood supplied to a compromised perfusion bed through the leptomeningeal arteries. This quantitative Local-AIF qCBF may be of benefit to studies of novel stroke therapeutics that would be influenced by collateral supply, and for translation to clinical CT perfusion.

DATA AVAILABILITY

All data and code are available upon request to the corresponding author.

ACKNOWLEDGMENTS

The authors would like to acknowledge the support of the US National Institutes of Health R01-NS093908 (Carroll/Christoforidis) and The National Science Foundation DGE-1746045 (Liu).

REFERENCES

1. Liebeskind DS, Saber H, Xiang B, et al. Collateral Circulation in Thrombectomy for Stroke After 6 to 24 Hours in the DAWN Trial. *Stroke.* 2022;53(3):742-748.
2. Winship IR. Cerebral collaterals and collateral therapeutics for acute ischemic stroke. *Microcirculation.* 2015;22(3):228-236.
3. Marks MP, Heit JJ, Lansberg MG, et al. Endovascular Treatment in the DEFUSE 3 Study. *Stroke.* 2018;49(8):2000-2003.
4. Shazeeb MS, King RM, Anagnostakou V, et al. Novel Oxygen Carrier Slows Infarct Growth in Large Vessel Occlusion Dog

Model Based on Magnetic Resonance Imaging Analysis. *Stroke.* 2022;53(4):1363-1372.

5. Christoforidis GA, Saadat N, Liu M, et al. Effect of early Sanguinate (PEGylated carboxyhemoglobin bovine) infusion on cerebral blood flow to the ischemic core in experimental middle cerebral artery occlusion. *J Neurointerv Surg.* 2022;14(12):1253-1257.
6. Saadat N, Christoforidis GA, Jeong YI, et al. Influence of simultaneous pressor and vasodilatory agents on the evolution of infarct growth in experimental acute middle cerebral artery occlusion. *J Neurointerv Surg.* 2020.
7. Liu M, Saadat N, Jeong YI, et al. Augmentation of perfusion with simultaneous vasodilator and inotropic agents in experimental acute middle cerebral artery occlusion: a pilot study. *J Neurointerv Surg.* 2023;15(e1):e69-e75.
8. Lee MJ, Son JP, Kim SJ, et al. Predicting Collateral Status With Magnetic Resonance Perfusion Parameters: Probabilistic Approach With a Tmax-Derived Prediction Model. *Stroke.* 2015;46(10):2800-2807.
9. Jeong YI, Christoforidis GA, Saadat N, et al. Absolute quantitative MR perfusion and comparison against stable-isotope microspheres. *Magn Reson Med.* 2019;0(0):1-11.
10. Mouannes-Srour JJ, Shin W, Ansari SA, et al. Correction for arterial-tissue delay and dispersion in absolute quantitative cerebral perfusion DSC MR imaging. *Magn Reson Med.* 2012;68(2):495-506.
11. Calamante F, Willats L, Gadian DG, Connelly A. Bolus delay and dispersion in perfusion MRI: implications for tissue predictor models in stroke. *Magn Reson Med.* 2006;55(5):1180-1185.
12. Rink C, Christoforidis G, Abduljalil A, et al. Minimally invasive neuroradiologic model of preclinical transient middle cerebral artery occlusion in canines. *Proc Natl Acad Sci U S A.* 2008;105(37):14100-14105.
13. Christoforidis GA, Rink C, Kontzialis MS, et al. An endovascular canine middle cerebral artery occlusion model for the study of leptomeningeal collateral recruitment. *Investigative radiology.* 2011;46(1):34-40.
14. Christoforidis GA, Vakil P, Ansari SA, Dehkordi FH, Carroll TJ. Impact of Pial Collaterals on Infarct Growth Rate in Experimental Acute Ischemic Stroke. *AJNR American journal of neuroradiology.* 2017;38(2):270-275.
15. Christoforidis GA, Mohammad Y, Kehagias D, Avutu B, Slivka AP. Angiographic assessment of pial collaterals as a prognostic indicator following intra-arterial thrombolysis for acute ischemic stroke. *AJNR American journal of neuroradiology.* 2005;26(7):1789-1797.
16. Carroll TJ, Rowley HA, Haughton VM. Automatic calculation of the arterial input function for cerebral perfusion imaging with MR imaging. *Radiology.* 2003;227(2):593-600.
17. Carroll TJ, Horowitz S, Shin W, et al. Quantification of cerebral perfusion using the "bookend technique": an evaluation in CNS tumors. *Magn Reson Imaging.* 2008;26(10):1352-1359.
18. Sakaie KE, Shin W, Curtin KR, McCarthy RM, Cashen TA, Carroll TJ. Method for improving the accuracy of quantitative cerebral perfusion imaging. *J Magn Reson Imaging.* 2005;21(5):512-519.
19. Shin W, Cashen TA, Horowitz SW, Sawlani R, Carroll TJ. Quantitative CBV measurement from static T1 changes in tissue and correction for intravascular water exchange. *Magn Reson Med.* 2006;56(1):138-145.
20. Shin W, Horowitz S, Ragin A, Chen Y, Walker M, Carroll TJ. Quantitative cerebral perfusion using dynamic susceptibility contrast MRI: evaluation of reproducibility and age- and gender-dependence with fully automatic image postprocessing algorithm. *Magn Reson Med.* 2007;58(6):1232-1241.
21. Vakil P, Lee JJ, Mouannes-Srour JJ, Derdeyn CP, Carroll TJ. Cerebrovascular occlusive disease: quantitative cerebral blood flow using dynamic susceptibility contrast mr imaging correlates with quantitative H2[15O] PET. *Radiology.* 2013;266(3):879-886.
22. Systems SM. Absolute quantitative DSC cerebral perfusion

imaging with SCALE-PWI. *N4_VD13D_1049_Z00387MF_QIAN_SCALEPWI.* 2015;WIP #1049.

23. *T1Bookend DSC Perfusion with global and local AIF open source code* [computer program]. Version 1.2.0. Github2024.
24. Shah MK, Shin W, Parikh VS, et al. Quantitative cerebral MR perfusion imaging: preliminary results in stroke. *J Magn Reson Imaging.* 2010;32(4):796-802.
25. Yaghi S, Khatri P, Prabhakaran S, et al. What Threshold Defines Penumbral Brain Tissue in Patients with Symptomatic Anterior Circulation Intracranial Stenosis: An Exploratory Analysis. *J Neuroimaging.* 2019;29(2):203-205.
26. Calamante F, Christensen S, Desmond PM, Ostergaard L, Davis SM, Connelly A. The physiological significance of the time-to-maximum (Tmax) parameter in perfusion MRI. *Stroke.* 2010;41(6):1169-1174.
27. Jones TH, Morawetz RB, Crowell RM, et al. Thresholds of focal cerebral ischemia in awake monkeys. *J Neurosurg.* 1981;54(6):773-782.
28. Nael K, Doshi A, De Leacy R, et al. MR Perfusion to Determine the Status of Collaterals in Patients with Acute Ischemic Stroke: A Look Beyond Time Maps. *American Journal of Neuroradiology.* 2018;39(2):219-225.
29. Federau C, Wintermark M, Christensen S, et al. Collateral blood flow measurement with intravoxel incoherent motion perfusion imaging in hyperacute brain stroke. *Neurology.* 2019;92(21).
30. Liu M, Saadat N, Jeong Y, et al. Quantitative perfusion and water transport time model from multi b-value diffusion magnetic resonance imaging validated against neutron capture microspheres. *Journal of Medical Imaging.* 2023;10(06).

APPENDIX

A1. Stroke Model

All experiments were conducted using a preclinical canine model of ischemic stroke[9,12,13]. The two-day experimental protocol was approved by the University of Chicago Institutional Animal Care and Use Committee and reported in compliance with ARRIVE guidelines. In this study, a series of 7 purpose bred adult canines (mean age = 4.1±2.9y, mean weight = 25.8±3.7kg, 6 female, 1 male) underwent permanent endovascular middle cerebral artery occlusion (MCAO) via embolic occlusion coils at the M1 segment with R/L randomized throughout the experiments. MCAO was then verified via selective ipsilateral and contralateral internal carotid and vertebral arteriography using a previously reported technique[5-7,13,14]. Vertebral and bilateral internal carotid arteriograms confirmed MCAO without involvement of other vessels and assessed pial collateral recruitment. Subjects underwent arteriography and all CBF assessment under general anesthesia.

Isoflurane (1% End-Tidal, 0.75 minimum alveolar concentration for canines), propofol infusion (6 mg/kg IV followed by continuous 0.1-0.2 mg/min), and intravenous rocuronium (0.4-0.6 mg/kg every 10-30 minutes) were used to maintain anesthesia with minimal influence on cerebral perfusion. Physiology was monitored via invasive blood pressure, End-Tidal CO_2, O_2 saturation, rectal temperature, heart rate, cardiac rhythm, arterial blood gases, glucose, electrolytes, and hematocrit. Pial collateral recruitment was quantified 30 minutes post-MCAO by assessing x-ray arteriographic images (OEC9800; General Electric Healthcare, Chicago, IL) as a pial collateral score (PCS)[14] blinded to CBF (Appendix A2. Pial Collateral Score). After deployment of the coil, subjects were transported to the MRI scanner for advanced physiologic imaging. Battery operated pumps and ventilators were affixed to the specially designed transport cart to maintain physiologic parameters within acceptable ranges throughout transport. In addition, real-time physiology monitoring (Heart Rate, BP, EtCO2, PaCO2) were also displayed to the veterinary staff for the duration of the imaging to identify any changes that would bias results.

The animals then underwent MRI DSC perfusion and serial quantification of infarct volume by DTI and were euthanized either the same evening or the following day. Those with unanticipated events such as abnormal baseline MRI, intraprocedural intracranial vessel perforation, or excessive deviation in physiologic parameters during MCAO (presumably from an unanticipated procedural related event) were excluded from this study.

A2. Pial Collateral Score

The 11-point canine pial collateral score was based on the premise shown in Christoforidis, GA et al. (2005) "Angiographic Assessment of Pial Collaterals as a Prognostic Indicator Following Intra-arterial Thrombolysis for Acute Ischemic Stroke", Am J Neuroradiol[15]. This prior publication provides figures for reference to calculate PCS in human patients. Adaptation of this scoring system for the preclinical canine model was done as follows.

Arteriograms (OEC 9800, GE Healthcare, Chicago, IL, USA) were acquired 30 min following occlusion. Collaterals were scored as follows: 3 points were given if collaterals extended over the surface of the brain to each of the 3 sections of the MCA territory (1 point was given if there was reconstitution of arteries identified over the anterior region of the MCA territory, a second for the middle region, and a third for the posterior region; up to 3 points). An additional point was given for each territory if there was reconstitution of branches along the lateral surface of the MCA territory to reach the distal M2 segments (up to 6 points). A point was given for angiographic reconstitution of the proximal M2 segments and another if this reached the junction of M1 and M2 segments (up to 8 points). Finally, another was given if there was minimal reconstitution of the MCA, a second if there was clear reconstitution of MCA branches, and a third if there were reconstitution along the lateral surface of the MCA to the distal M2 branches (up to 11 points). The 11-point canine pial collateral score Bland-Altman statistic was 22.6%, indicating that 95% of calculated scores were within a factor of 1.3 of each other for two observers[13]. Mean difference between two observers for pial score was 0.23 (σ=0.69) for a mean score of 5.9 and an individual intraclass correlation of 0.98[13].

A3. Local-AIF Model

When contrast is injected via IV, it travels through the heart and lungs and finally to the circle of Willis before perfusing the brain. In dynamic susceptibility contrast MRI, the shape of contrast bolus upon entering the brain represents a Global arterial input function (Global-AIF). This means that contrast is not an instantaneous delta function despite treating it as a surrogate of unit impulse of blood flow. The capillary bed can be modeled as a linear system and the arterial input function (AIF) modeled as a sum of time-shifted and scaled direct delta function inputs as shown in Eq. 1

$$[Gd](t) = CBF \times Global\text{-}AIF \otimes R(t) \quad (1)$$

The fraction of gadolinium contrast [Gd] in the tissue at time t after the delta input is the residue function $R(t)$. Since the AIF is not instantaneous to every voxel, it is dispersed in time as a curve as the bolus travels through the capillary network. This can be represented as a set of Dirac delta functions at different time delays as a convolution of the Global-AIF with the residue function.

When there is an occlusion of a major artery, blood will have to travel around the occlusion to reach the infarcted hemisphere; the delay and the dispersion as blood travels through the collateral network can be corrected for with a Local-AIF. The Local-AIF model treats the brain as two elements in a delay and dispersion term that account for the late arrival and additional "blunting" of the bolus shape as it propagated through the brain. This is known as a cascade interconnected linear time-invariant system with an added time shift operator

(delay) and dispersive element (dispersion). The delay and dispersion term is based on the delay of the bolus arrival and the strength of the bolus dispersion as measured from between the Global-AIF and the venous outflow (VOF) through the sagittal sinus. The dispersion function depends on the time of arrival in the tissue and imparts zero dispersion on prompt arrival.

With a selection of the Global-AIF based on automatic early arrival time and narrow bolus, and selection of VOF in the sagittal sinus, the strength of delay and dispersion based on arrival time can be calculated as α and β as a function of the time delay t_D between Global-AIF and VOF.

$$VOF(t + t_D) = \frac{\alpha}{(t_D + 1)} e^{-\frac{\beta t}{t_D}} \otimes Global\text{-}AIF(t) \tag{2}$$

The Local-AIF for every voxel with a voxel-specific delay of Δt can be found by deconvolving the Global-AIF and the residue function of the VOF using the fit parameters α and β from Eq. 2 to return the quantitative Local-AIF qCBF.

$$Local\text{-}AIF(t) = Global\text{-}AIF(t - \Delta t) \otimes \frac{\alpha}{(\Delta t + 1)} e^{-\frac{\beta t}{\Delta t}} \tag{3}$$

From this Local-AIF qCBF can be calculated on a voxel-wise basis with delay and dispersion correction to capture collateral supply in territories distal to an occlusion by correcting Eq. 1.

Deconvolution of Eq. 4 will return the Local-AIF qCBF.

$$[Gd](t) = Local\text{-}AIF\ qCBF\ \times\ Global\text{-}AIF(t) \otimes \frac{\alpha}{(\Delta t + 1)} e^{-\frac{\beta t}{\Delta t}} \otimes R(t) \tag{4}$$

This method is fully automated to minimize user bias[20], and is available for use with both a Global-AIF and a Local-AIF[22,23].